Am J Transl Res 2019;11(5):2866-2876
www.ajtr.org /ISSN:1943-8141/AJTR0090280

Original Article

Transplantation of HUVECs with genetically modified Nogo-B accelerates wound-healing in nude mice

Xingtong Wang[1*], Yongjun Zheng[2*], Haibin Wu[4*], Song Tian[2], Minjuan Wu[3], Pengfei Luo[2], Fang Zhang[2], He Fang[2], Hengyu Li[5], Zhaofan Xia[2]

[1]Department of Burns and Plastic Surgery, Sixth Medical Center of General Hospital, The People's Liberation Army, Beijing 100046, China; [2]Burns Center of Changhai Hospital, [3]Department of Histology and Embryology, The Second Military Medical University, Shanghai 200433, China; [4]Department of Burns and Plastic Surgery, General Hospital of Central Theater Command, The People's Liberation Army, Wuhan 430070, China; [5]The Fourth Department of General Surgery, Changhai Hospital, Second Military Medical University, Shanghai 200433, China. [*]Co-first authors.

Received December 22, 2018; Accepted March 8, 2019; Epub May 15, 2019; Published May 30, 2019

Abstract: Wound repair is an intractable problem in clinic, with limited treatment options. Previous studies have demonstrated the therapeutic potential of Nogo-B in tissue repairs. However, the therapeutic effect of Nogo-B in HUVEC is still unknown. In this study, we examined the benefit of genetically modified Human Umbilical Vein Endothelial Cells (HUVECs) and found that down regulation of Nogo-B significantly promoted secretion of growth factors involving in wound healing and greatly boosted the proliferation, migration of fibroblasts and epithelial cells. Moreover, using an excisional wound splinting model, we showed that injection of exogenous HUVEC-siNogo-B around the wound significantly enhanced angiogenesis and wound healing in nude mice. Thus, our data suggests that genetically modified HUVECs support microenvironment suitable for wound healing and systemically demonstrates the beneficial effect of HUVECs in wound healing.

Keywords: Nogo-B, human umbilical vein endothelial cells (HUVECs), angiogenesis, paracrine, wound healing, nude mice

Introduction

Cutaneous wound healing requires a well-orchestrated integration of the complex biological and molecular events of cell migration, proliferation, extracellular matrix (ECM) deposition, angiogenesis, and remodeling [1]. The variety of cytokines and growth factors play a key role in wound healing by activating signaling pathway for other cells, mainly including keratinocytes and fibroblasts, thus initiating migration and proliferation of these cells [2]. The ways of boosting wound healing includes regulating inflammation, accelerating granulation, angiogenesis and re-epithelization. Previous studies mostly focus on one of them. Researchers have attempted to apply various growth factors such as vascular endothelial growth factor (VEGF) or human dermal fibroblasts (HDF) onto wounds to promote angiogenesis and wound healing [3, 4]. There is still no comprehensive method to affect the wound healing process. Recently there is substantive evidence that the endothelial cells retain a stem cell potentiality and its secretome was able to prime adipose-derived stem cells for improved wound healing in diabetes. It is also able to differentiate into mesenchymal components which could secrete cytokines affecting angiogenesis and proliferation of fibroblasts and epithelial cells [5, 6]. However, how to regulate endothelial cells to enhance its paracrine is not reported.

The Nogo-B is one of members of the Nogo protein family, and is highly expressed in most tissues to regulate vascular remodeling, cell proliferation, acute inflammation and tissue repair. Inendothelial and smooth muscle cells, Nogo-B acts as a regulator to promote the migration of endothelial cells but inhibit migration of vascular smooth muscle cells, which is a process necessary for vascular remodeling [7]. In the

liver, Nogo-B is mainly expressed in nonparenchymal cells and promotes hepatocyte proliferation by facilitating the IL-6/STAT3 signaling pathway [8]. During pulmonary inflammation, Nogo-B protects mice against lipopolisaccharide-induced acute lung injury through the modulation of alveolar macrophage recruitment and PTX3 production [9]. Furthermore, it is reported that Nogo-B(-/-)mice exhibit defects in macrophage recruitment and reduced arteriogenesis and blood flow recovery after injury [10]. However, how Nogo-B itself contributes to wound healing is not yet fully understood.

In this study, we transducted GV248-Nogo-B-RNAi-GFP in Human Umbilical Vein Endothelial Cells (HUVECs) to explore how Nogo-B affect proliferation of HUVECs, tube formation and the paracrine of cytokines. Then we collected the supernatant of Nogo-B(-/-) HUVECs to detect whether the conditioned medium could enhance the proliferation and migration of fibroblasts and epidermal cells. Finally we injected Nogo-B(-/-) HUVECs intradermally into excisional wounds in nude mice and explored their benefit on wound healing.

Materials and method

Cell culture

Human umbilical vein endothelial cells (HUVECs) were purchased from ScienCell (San Diego, USA) and cultured in endothelial cell medium (ECM, Gibco, Life Technologies) supplemented with 10% FBS. HUVECs between passages 2 and 4 were used for cell experiments.

Cell transfection

We chose the Nogo-B interference sequence as: CAGAATCTATGGACTGAAT [10].

The DNA sequence in recombinant plasmid was here: GIDL29193-RNAi (9525-1)-a: CCGGCACAGAATCTATGGACTGAATCTCGAGATTCAGTCCATAGATTCTGTGTTTTTG; GIDL29193-RNAi (9525-1)-b: AATTCAAAAACACAGAATCTATGGACTGAATCTCGAGATTCAGTCCATAGATTCTGTG.

After annealing into double-stranded DNA, and connecting to the virus carrier GV248, then we build the recombinant lentivirus vector GV248-Nogo-B-RNAi-GFP.

The HUVECs (2-4 passages) were transfected with green fluorescent protein (GFP)-labeled Nogo-B-RNAi-GFP or GFP alone to obtain GFP-labeled HUVEC-siNogo-B or GFP-labeled (HUVEC-NC). The amount of relative expression of Nogo-B mRNA was detected by Real Time RT-PCR and analyzed by the $2^{-\Delta\Delta CT}$ method using HUVECs without LV transfection as the reference. The transfection rate was defined as the ratio of the number of GFP cells to the number of total cells and analyzed by flow cytometry.

Measurement of levels of cytokines in supernatant by protein array

Transfected HUVECs were cultured in 10 cm plate and changed medium to DMEM when cells grew in 70%-80% confluence. After 24 h, the supernatant were collected. Level of cytokines in supernatant were measured by protein array (Shanghai Biotechnology Co., Ltd., China) according to the instruction manuals.

HUVECs network formation assay

2.5×10^4 HUVECs were suspended in 0.4 ml of epithelial growth medium (EGM)-2 basal medium supplemented with 5% FBS. HUVEC-NC and HUVEC-siNogo-B were seeded onto Matrigel (BD Biosciences)-coated 96-well plates; and incubated at 37°C/5% CO_2 for 6 hours. After removal of the medium, the cells were fixed, and images were captured. The quantity of the tube-like structures was calculated. Three random fields were measured for each well.

Flow cytometry

For detection of GFP-positive cells in the wounded skin, excised wounds together with a small amount of surrounding skin were dispersed into single-cellsuspensions. In brief, the tissue was minced, and incubated in a digestion buffer containing hyaluronidase (1 mg/ml), collagenase D (1 mg/ml), and DNAse (150 units/ml) in a 37°C shaking water bath for 2 hours. The collagenase and the hyaluronidase digests were pooled and filtered through a 70 um nylon cell strainer. Cells were pelleted and resuspended in PBS and analyzed for GFP-positive cells using Flow Cytometer (Beckman, Los Angeles, CA, USA). Cells from sham wounds were used as negative controls.

Fluorescence detection

HUVECs in their 3rd passage were transfected with GV248-Nogo-B-RNAi-GFP using enhanced

infection solution and were cultured in DMEM (DMEM-LG; Gibco, Invitrogen) supplemented with 10% FBS (Gibco, Invitrogen). At passage 2-4 were analyzed for purity and epitope expression using fluorescence-activated cell sorting (FACS) analysis. In the nude mice, after being harvested, lesion tissues were bisected and fixed in 4% paraformaldehyde containing 10% sucrose at 4°C for 12 h and then 30% sucrose for 24 h. The specimens were then embedded in OCT compound and stored at -80°C until use. They were cut at 10 μm mounted onto Super Frost-Plus charged slides (Citotest, Jiangsu, China), and washed three times with PBS. After being air-dried for 10 min, they were subjected to 4',6-diamidino-2-phenylindole (DAPI) (1 μg/ml; Sigma-Aldrich) for nuclear-staining and photographed with fluorescence microscopy.

Proliferation and migration

HUVEC-NC and HUVEC-siNogo-B were cultured in 10 cm plate and then changed medium to DMEM when cells grew in 70%-80% confluence. After 24 h, the supernatant were collected. For wound scratch assay, fibroblasts and epidermal cells (1.0×10^6) were plated in 6-well plates, and after 24 h, drew a line in the middle of each well with 200 ul pipette tip. In the meanwhile, we changed the medium to DMEM, 50% HUVEC-NCsuper-natant, 50% HUVEC-siNogo-B supernatant, and captured the images with microscope (Leisa, German) in different time points. Wound area was carried out by Image-J software. For proliferation assay, fibroblasts and epidermal cells (1000 cells/well) were seeded in 96-well plate, while after 24 h, changed the medium to DMEM, 50% HUVEC-NCsupernatant, 50% HUVEC-siNogo-B supernatant and 5% FBS (each group had triplicate wells), add CCk-8 regent (Beyotime, China), and incubated in 37°C for 3 h, then absorbance were detected by Multiscan Spectrum (Biorad, USA). Continuous observation lasted for 7 days. Each test had triplicate experiments for statistics analysis.

For Transwell assay, three medium groups (DMEM, 50% HUVEC-NC and 50% HUVEC-siNogo-B) were added to the lower chamber of 24-well Transwell (8 μm pore size, Corning, USA), fibroblasts (1×10^5) were cultured in the upper chamber by keeping the fluid surfaces of the lower and upper chambers at the same level. After 24 h culture, the filters were fixed and stained with crystal violet (0.1% Sigma, USA), photographed, and counted using Leica Q-Win image analysis software. Experiments were carried out in triplicate and repeated at least three times.

Animals, wound model, and treatment

Institutional approval of the protocol was obtained and all animal experiments were performed according to the NIH Animal Care & Use Guidelines and the institutional animal care and use committee of the Second Military Medical University, shanghai, China. The nude mice (6-8 weeks, purchased from Slac Laboratory Animal Co. Ltd, Shanghai, China) were anesthetized with 1% sodium pentobarbital intraperitoneally. Two full-thickness 8 mm excisional splint wounds were inflicted on the dorsal skin of each mouse [11]. HUVECs were harvested at the third passage and suspended in low-glucose DMEM for injection. HUVEC-siNogo-B (1.0×10^6) in 0.2 ml of DMEM was slowly and carefully injected into the center of each lesion from the edge of the wound with a 29-G needle. Similarly, 0.2 ml of HUVEC-NC or DMEM was injected into each lesion in the same way. Repeat injection once more in 48 h. Photographs were taken regularly from a certain distance after treatment. The mice were randomly assigned to three groups: Control, HUVEC-NC and HUVEC-siNogo-B. The wound area was measured 3, 5, 7, 10 and 14 days after injection in all groups using Image-Pro Plus Software, and the wound healing rate was calculated using the following equation: would healing rate = (original wound area - current wound area)/original wound area ×100%.

Tissue harvesting in mice

The skin tissue was collected on day 3, day 5, day 7 and the wounds were excised with the wound margins. For fluorescence detection, the tissue embedded with OCT and frozen section were performed. For hematoxylin and eosin staining and immunohistochemistry (IHC) staining in paraffin, the tissue was fixed in 10% formalin for 24 hours and embedded in paraffin.

Wound healing assays

Wound healing rate was assessed on day 3, day 5, day 7, day 10 and day 14 after wounding. Re-epithelialization was measured by histomorphometric analysis of sections taken from the

center of the wound and stained with hematoxylin and eosin. Images were obtained using a digital camera (Sony, Japan), and analyzed using Image-Pro Plus Software. The percentage of re-epithelialization [(distance traversed by epithelium over wound from wound edge/distance between wound edges) ×100] was calculated for two sections per wound and was averaged over sections to provide a representative value for each wound.

Histologic staining

Tissue specimens were fixed in 4% paraformaldehyde for 24 h and embedded in paraffins. Six-micron-thick sections were stained with H&E for light microscopy. Besides, the paraffin sections were routinely dewaxed, rinsed, incubated with 4% fetal bovine serum (Gibco, Gaithersburg, MD, USA) for 1 h, and then incubated with corresponding monoclonal antibodies against CD31 (1:200, Abcam, Cambridge, UK) at 4°C overnight. The primary antibodies were detected with horseradish peroxidase (HRP)-labeled antibodies (1:300, Santa Cruz) and visualized with diaminobenzidine (Boster, Wuhan, China). The slides were examined and photographed under afluorescencemicroscope (Leisa, German).

Western blotting

2.0×10^5 HUVECs were extracted in 150 ul cell-lysis buffer (CST, USA) containing proteinase inhibitors (Bio Tools, USA). Lysates were centrifuged at 12,000 rpm for 15 minutes at 4°C, and the supernatants were collected for Western blot analysis. Protein concentration of the supernatants was determined by BCA protein assay kit. Samples were separated on 10% SDS-polyacrylamide gel and transferred to nitrocellulose membranes. Membranes were incubated overnight at 4°C with monoclonal antibody against Nogo-B (CST, USA). Then the membranes incubated with horseradish peroxidase (HRP)-labeled second antibodies (1:2000, Santa Cruz) in room temperature for 1 h. The membrane detected by automatic exposure.

Statistical analysis

Data statistical analysis was performed by SPSS16.0, and the results of normal distribution and homogeneity of variance were expressed as mean ± SD. Statistical analysis was carried out using paired 2-tailed Student's t-test or one-way ANOVA procedures. Values of $P<0.05$ were considered statistically significant.

Results

Nogo-B affect HUVECs proliferation, tubes formationa and paracrine

The primary HUVECs grew well and shaped like spindles with no vacuole seen in the cytoplasm. After transfected with GV248-Nogo-B-RNAi-GFP, the most fluorescent signal was concentrated in the cytoplasm (**Figure 1A**). Western Blotting showed Nogo-B expression was completely inhibited by the action of RNAi (**Figure 1B**). CCK-8 Assay was performed to investigate the effect ofdown regulating Nogo-Bon the proliferation of HUVECs. The HUVEC-siNogo-B group grew significantly lower than HUVEC-NC group from 24 h to 72 h (**Figure 1C**). In order to determine the effect of down regulating Nogo-B expression of HUVECs on its exvivo angiogenic capacity, we examined the tube formation of HUVECs in Matrigel. We found that HUVEC-siNogo-B group significantly suppressed HUVEC tube formation on Matrigel compared with NC control. As is shown in **Figure 1D**, the HUVEC-siNogo-B group (5.6±0.6782) generated less vascular ring than the HUVEC-NC group (15± 1.414, $***P<0.001$, n=5). Moreover, The supernatant of HUVEC-NC and HUVEC-siNogo-B were collected after 24 hours of culture and Antibody microarray analysis was performed (**Figure 2A**). We found that the pro-healing cytokines of EGF, VEGF-D, Progranulin and FGF-4 in the HUVEC-siNogo-B supernatant were increased 2-fold when compared to the HUVEC-NC supernatant. Whereas, the pro-inflammation cytokines of TLR4, MCP-3 and anti-healing cytokines of VEGI, MMP-19 were decreased. (**Figure 2B**). Taken together, these results illustrated that Nogo-B could impact the proliferation and tube formation of HUVECs. When Nogo-B was knocked down in HUVECs, we found paracrinecytokines involved in promoting granulation formation and re-epithelization were greatly up-regulated, while the pro-inflammation cytokine sand anti-healing cytokines were suppressed.

HUVEC-siNogo-B-CM enhances migration and proliferation of fibroblasts and epidermal cells

HUVEC-siNogo-B supernatant was collected as conditioned medium. Migration and prolifera-

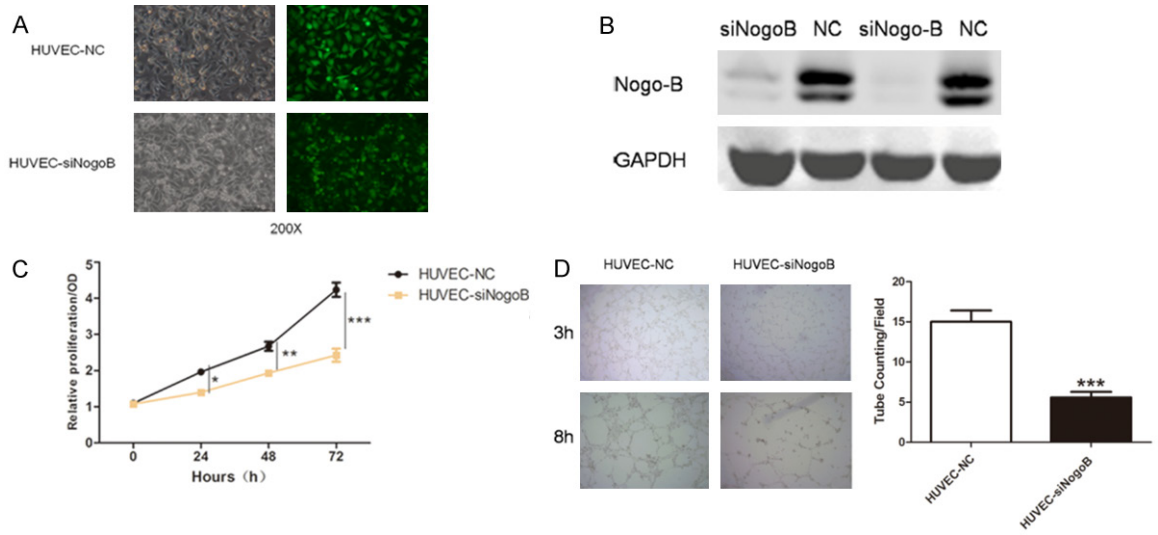

Figure 1. Nogo-B affected HUVECs proliferation and tube formation by transfected with GV248-Nogo-B RNAi-GFP. (A) The cells grew well and shaped like spindles with no vacuole seen in the nucleus and were transfected under a fluorescence microscope and the whole cell emits fluorescence (200X). (B) Detection of the Nogo-B expression by Western Blot. Nogo-B was completely knocked down. (C) The effect of Nogo-B on proliferation and (D) tube-formation of HUVECs were measured by CCk-8 assay and tube formation assay. Data was shown as means ± SD, (C) n=3; (D) n=5; **P*<0.05, ***P*<0.01, ****P*<0.001. Scar bars: 100 μm.

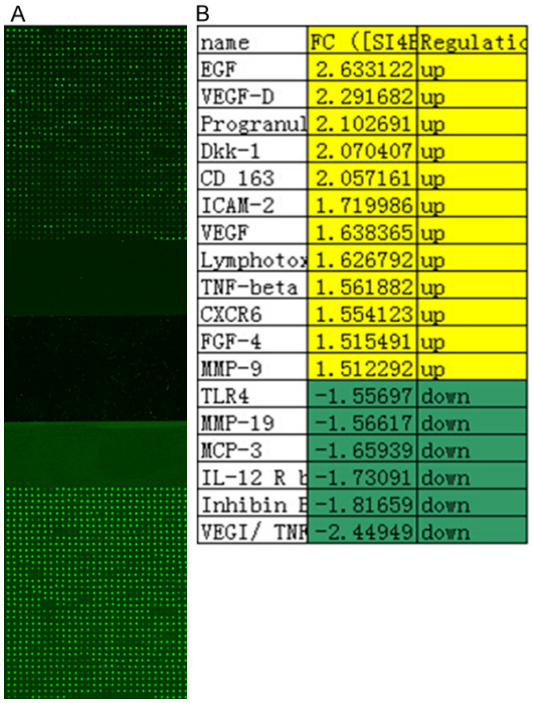

name	FC ([SI4E	Regulatic
EGF	2.633122	up
VEGF-D	2.291682	up
Progranul	2.102691	up
Dkk-1	2.070407	up
CD 163	2.057161	up
ICAM-2	1.719986	up
VEGF	1.638365	up
Lymphotox	1.626792	up
TNF-beta	1.561882	up
CXCR6	1.554123	up
FGF-4	1.515491	up
MMP-9	1.512292	up
TLR4	-1.55697	down
MMP-19	-1.56617	down
MCP-3	-1.65939	down
IL-12 R b	-1.73091	down
Inhibin B	-1.81659	down
VEGI/ TNF	-2.44949	down

Figure 2. Cytokines detected in HUVECs supernatant after knocked down Nogo-B. A. Cytokines in supernatant of HUVEC-NC and HUVEC-siNogo-B detected by antibody microarray. They were labeled by Cy3 and Cy5, which were two different fluorescent molecular. B. It showed the ratio of siNogo-B/NC from antibody microarray. EGF, VEGF-D, FGF-4 and Progranulin were increased obviously in the HUVEC-siNogo-B supernatant, whereas anti-angiogenesis cytokines MMP-19 and VEGI declined.

tion were measured with Scratch Test (**Figures 3A**, **4A**). Transwell Assay (**Figure 3C**) and CCk-8Assay (**Figures 3D**, **4C**), respectively. We found that the number of migrated fibroblasts in the 50% HUVEC-siNogo-B-CM was significantly greater than that in the 50% HUVEC-NC-CMin 24 h (*P<0.05, **Figure 3B**). Transwell test showed that the migration ability of chemotaxizing fibroblasts significantly increased by co-culture with 50% HUVEC-siNogo-B-CM. The number of crystal violet staining was 3-fold higher than in the 50% HUVEC-NC-CM group (98±4.41 *vs* 28.33±2.028, *P*<0.001) (**Figure 3C**). Moreover, the CCK-8 assay showed that the proliferative activity of fibroblasts increased markedly in 50% HUVEC-siNogo-B-CM as compared with 50% HUVEC-NC-CM group after 4 days of co-culturing (*P*<0.001) (**Figure 3C**). The same tendency as the epidermal cells performed (**Figure 4B**, **4C**). These results indicated that HUVEC-siNogo-B-CM greatly enhance the migration and proliferation both in fibroblasts and epidermal cells. At least three independent experiments were performed for analyses.

HUVEC-siNogo-B treated wounds exhibited faster wound closure

To determine whether HUVECs could survive by intradermally injected around the wound, the flow cytometry (**Figure 5A**) and the Immuno-

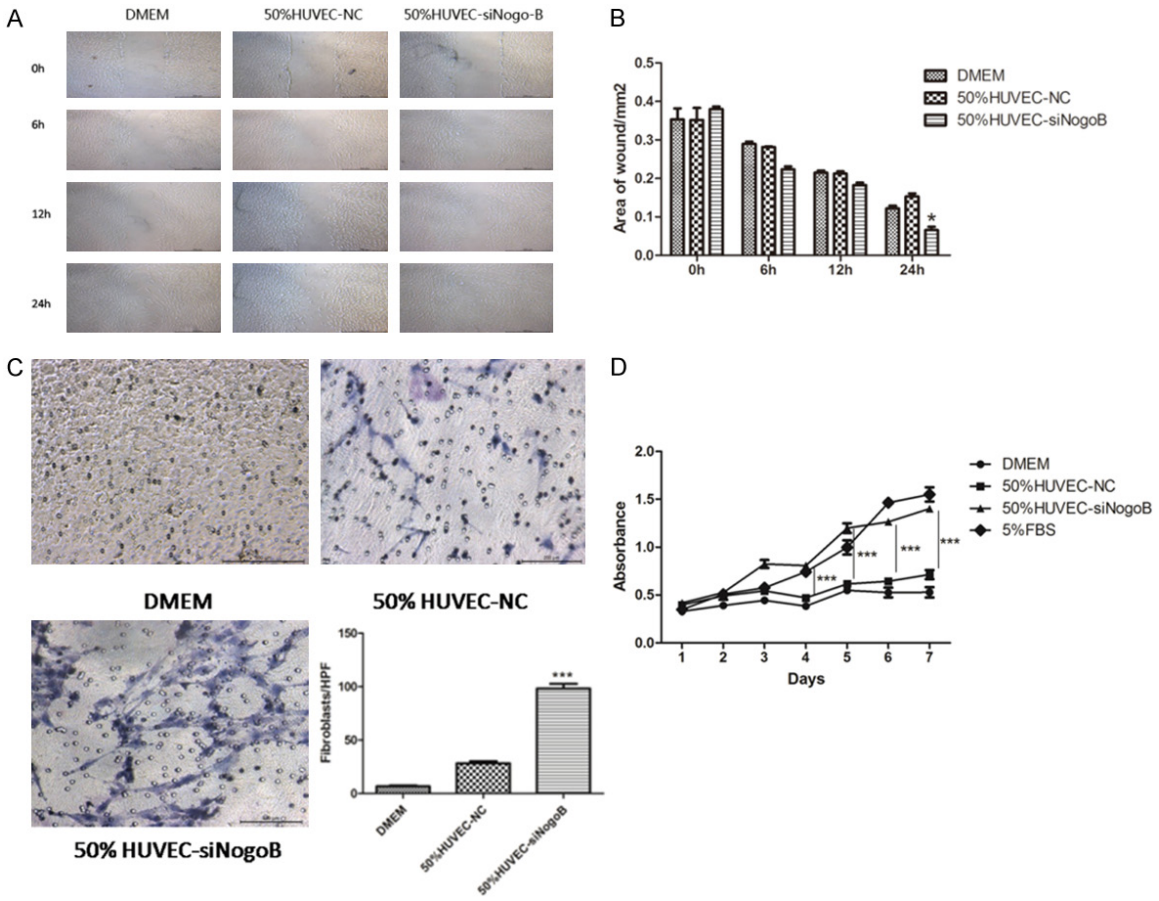

Figure 3. HUVEC-siNogo-B-CM exhibited chemoattractive, mitogenic effects on fibroblasts. (A, B) The pictures showed the scratch test of fibroblasts in 24 h. The number of migrating fibroblasts in 50% HUVEC-siNogo-B group was significantly greater than that in 50% HUVEC-NC group in 24 h the migration (C) and proliferation (D) of fibroblasts were measured by Transwell Assay and CCk-8 Assay. The proliferative activity of fibroblasts increased markedly in 50% HUVEC-siNogo-B group as compared with 50% HUVEC-NC group after 4 days of co-culturing. Data was shown as means ± SD, n=3, **P*<0.05, ****P*<0.001. The scale bar is 500 μm.

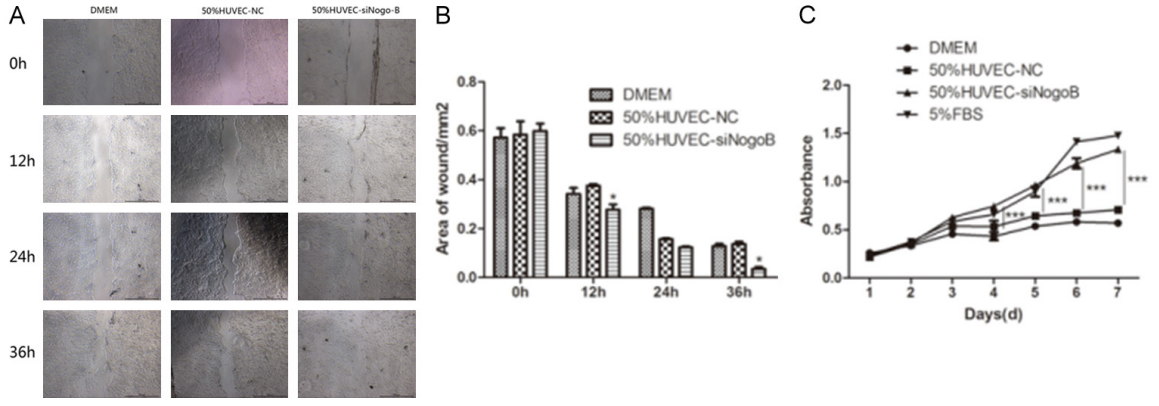

Figure 4. The HUVECs-siNogo-B-CM promoted migration of epidermal cells. The migration of epidermal cells was measured by scratch test (A, B) and CCk-8 Assay (C). The epidermal cells in the 50% HUVEC-siNogo-B group was significantly greater than that in the 50% HUVEC-NC group in 12 h and 36 h. The scale bar is 500 μm. The epidermal cells in 50% HUVEC-siNogo-B group increased significantly faster after 4 days co-culturing. 5% FBS was treated as positive control and HUVEC-NC, DMEM as negtive control. Data was shown as means ± SD, n=3; **P*<0.05, ****P*<0.001. The scale bar is 500 μm.

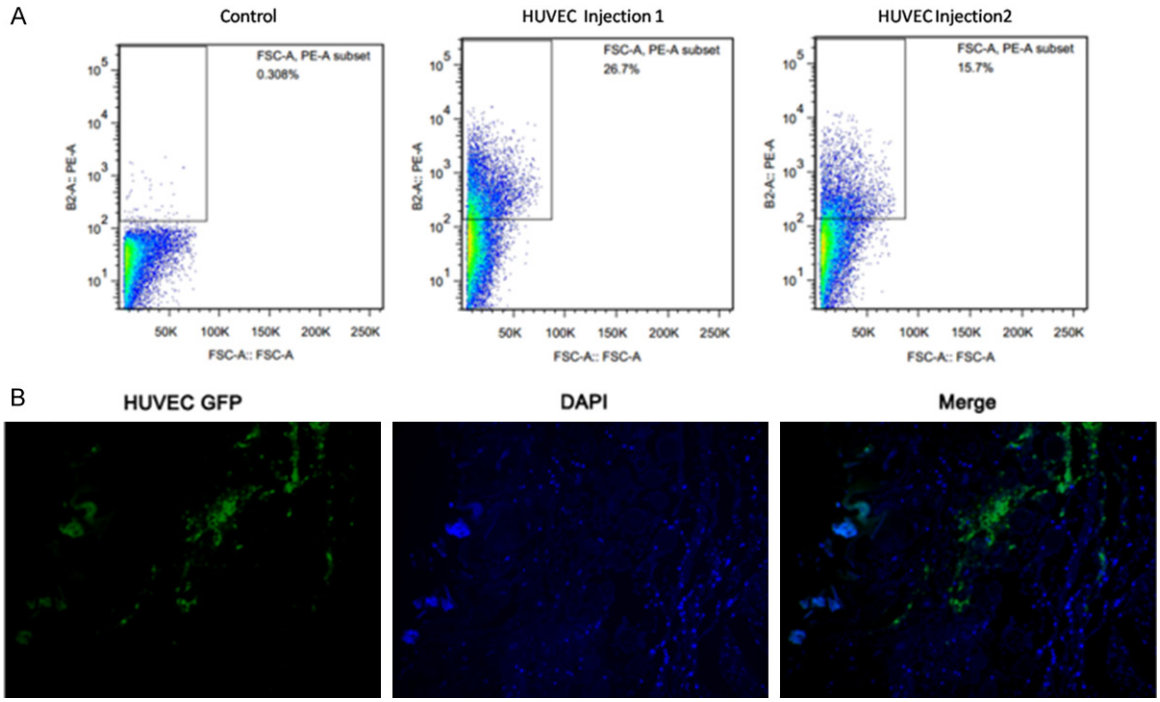

Figure 5. HUVEC-siNogo-B could survive in 48 h after injected intradermally around the excisional wound on mice. The flow cytometry and the Immunofluorescence were performed to detected the survival of HUVEC-siNogo-B (GFP^+) cells. The blue spots in the top left corner represents alive cells (A). The quantity of blue spots in two injection groups was much higher compared with vehicle control group. (B) Representative immunofluorescent staining of The GFP-labeled HUVECs. GFP^+DAPI^+ were survival cells by initially injected.

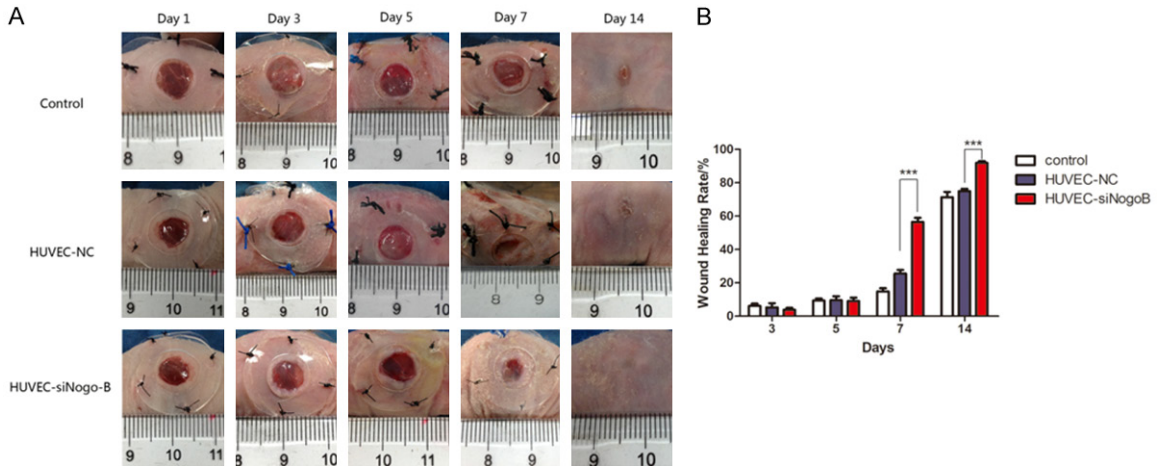

Figure 6. Topical administration of HUVEC-siNogo-B accelerated wound healing on mice. A. The wound was treated with saline, HUVEC-NC and HUVEC-siNogo-B, examined at day 1, day 3, day 5, day 7, day 14 after wounding and digitally photographed. B. Quantitative analysis of wound closure demonstrating higher wound healing rate in the HUVEC-siNogo-B group. Data was shown as means ± SD, n=6; ***P<0.001.

fluorescence (**Figure 5B**) were performed to detected the survival of HUVEC-siNogo-B (GFP^+) cells. The results showed that the HUVEC-siNogo-B could survive at least 5 days. Then we treated wound with saline, HUVEC-NC and HUVEC-siNogo-B, examined at day 1, day 3, day 5, day 7, day 14 after wounding (**Figure 6A**).

At day 7, and day 14, the corresponding wound healing rate were 56.478±2.508% and

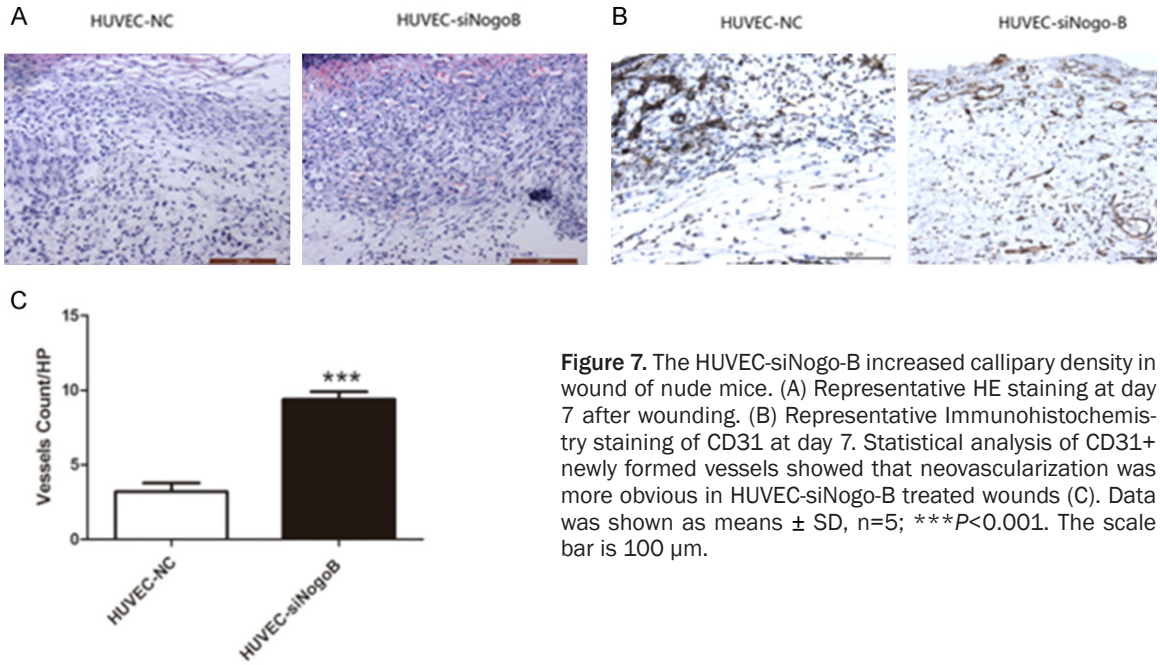

Figure 7. The HUVEC-siNogo-B increased callipary density in wound of nude mice. (A) Representative HE staining at day 7 after wounding. (B) Representative Immunohistochemistry staining of CD31 at day 7. Statistical analysis of CD31+ newly formed vessels showed that neovascularization was more obvious in HUVEC-siNogo-B treated wounds (C). Data was shown as means ± SD, n=5; ***P<0.001. The scale bar is 100 μm.

91.893±1.086% in the HUVEC-siNogo-B group, compared with 25.512±2.229% and 74.937±1.457% in the HUVEC-NC group (P<0.001). These results indicated that the wound healing rate in the HUVEC-siNogo-B group was significantly higher than that in the HUVEC-NC group.

The HUVEC-siNogo-B increased callipary density in wound of nude mice

HE staining was performed and we found the number of newly formed vessels in HUVEC-siNogo-B treated wounds was more than HUVEC-NC group at day 7 (**Figure 7A**). CD31 was a blood vessel endothelium cell marker and Immunohistochemistry staining of CD31 demonstrated that newly formed vessels in the HUVEC-siNogo-B group were more obvious than that in the HUVEC-NC group at day 7 wound of nude mice (**Figure 7B**). Capillary density in HUVEC-siNogo-B treated wound was 9.4±0.5099/HP, whereas the number was 3.2±0.5831/HP in the HUVEC-NC group (P<0.001, **Figure 7C**).

Discussion

Wound healing is a common problem faced by clinicians despite few curative options at hand. Innovative treatments to enhance wound healing and regeneration are needed. In the present experiment, we firstly found that down-regulation of Nogo-B could suppress the proliferation of HUVECs and tube formation, but increased paracrine signaling. Reverse-phase microarray analysis showed that positive cytokines involved in wound healing such as EGF, VEGF, FGF and Progranulin were greatly up-regulated while the negative regulators of angiogenesis like Vascular Endothelial Growth Inhibitor (VEGI), IL-12, MMP-19 as well as pro-inflammatory cytokines like MCP-3 and TLR-4 were decreased. We then performed injection of HUVEC-siNogo-B cells into an excisional wound in nude mice and found them significantly promote wound healing.

Nogo-B has been predominantly studied in oncologic [12-15], cardiovascular [7, 16-19], hepatic [8, 20-23] and lung diseases [24, 25] as well as in renal tubular epithelial cells [26]. In our study, we utilized lentiviral transduction to perform RNA interference in HUVECs and found that down-regulating Nogo-B could inhibit proliferation of HUVEC and tubes formation, but greatly changed the paracrine. It is quite similar with a previous study reported that Nogo-B is highly expressed in monocytes/macrophages and Nogo-B(-/-) monocytes are defective in cell migration and spreading [10]. Moreover, our data is a support of Nogo-B's role in increasing cell adhesion and promotion of endothelial cell migration [7]. Because Nogo-B is known as a role of inhibiting endovascular

hyperplasia, this might explain the observation that Nogo-B(-/-) in HUVECs generated positive cytokines involved in angiogenesis and wound healing.

Fibroblasts are the main cell component in the connective tissue of the dermis, and play an important role in collagen formation during the process of wound healing and a key role in wound closure andangiogenesis [27, 28]. Mutual contacts and interactions between fibroblasts and endothelial cells are important factors affecting angiogenesis [29]. In present experiment, we found that the supernatant of HUVEC-siNogo-B greatly promoted the proliferation, migration of fibroblasts and epidermal cells owing toup-regulating of EGF, FGF and Progranulin, which is a secreted glycoprotein directly activated proliferation and migration on fibroblasts and epidermal cells [30].

It is reported that Nogo-B is up-regulated in response to ischemia and necessary for blood flow recovery secondary to ischemia and wound healing linked to macrophage infiltration and inflammatory gene expression in vivo [10]. Different from the above finding, our study showed a variation of local wound affected by HUVEC-siNogo-B. In this study, we demonstrated that HUVEC-siNogo-B had significantly accelerated the wound closure and capillary density, suggesting that down-regulated Nogo-B in HUVECs promoted angiogenesis and wound healing notably. It is reported that Progranulin acts directly on dermal fibroblasts and endothelial cells to promote division, migration and the formation of capillary-like tubule structures [31]. As the **Figure 2B** showed, expression of VEGF and Progranulin were about 2.5-fold higher while VEGI and MMP-19 were lower than HUVEC-NC group. VEGI and MMP-19 are both negative regulator of endothelial cell [32]. These results may result in more angiogenesis expressed in HUVEC-siNogo-B treated mice. Moreover, granulation tissue is a crucial step in wound closure. As we could see from **Figure 7A** in the 7 days post after surgery, granulation tissues grew much faster in HUVEC-siNogo-B group. The mechanism might lie on the higher production of Progranulin and FGF secreted by HUVEC-siNogo-B. In the similar way, Up-regulated EGF may promote the proliferation and migration of epidermal cells, which might explain faster re-epithelization of cutaneous wound in the HUVEC-siNogo-B treated mice. Thus, it canbe speculated that down-regulated Nogo-B in HUVECs promoted wound healing through secreted multiple cytokines.

We did not follow up the survival of HUVECs for a long time. HUVECs do not express MHC-II-like antigens and possess weak immunogenicity. Therefore, we suggest that HUVECs would not induce significant rejection after injection and could survive in wounds. Previous study showed that the long-term survival of exogenously engrafted HUVECs remains 8.1% of the transplanted cells on day 14 [33]. Although the above findings suggest that allogenous HUVECs can survive in wounds for a long period of time, further studies are still necessary to determine the fate of HUVECs after injection into wounds.

In conclusion, this study systemically demonstrates the beneficial effect of HUVECs on cutaneous regeneration and wound healing in nude mice through paracrine effects. Down-regulating Nogo-B in HUVECs may ameliorate the microenvironment through paracrine of multiple cytokines, which may represent novel approaches in the angiogenesis of tissue engineering.

Acknowledgements

This work was funded by National Nature Science Foundation of China (81120108015, 81201443, 81701905), National Basic Research Program of China (973 Program, 2012CB518100), “Twelfth Five-Year” Scientific Program of China (AWS11J008, AWS14C001, 201502028), and the Shanghai Pujiang Program (17PJD043). Besides, especially thank editing work of Phillip Sanchez from Johns Hopkins University, School of Medicine.

Disclosure of conflict of interest

None.

Address correspondence to: Dr. Hengyu Li, The Fourth Department of General Surgery, Changhai Hospital, Second Military Medical University, Shanghai, China. Tel: +86-21-31161646; Fax: +86-21-65589829; E-mail: drlhy@foxmail.com; Dr. Zhaofan Xia, Burns Center of Changhai Hospital, The Second Military Medical University, Shanghai, China. Tel: +86-21-31161821; Fax: +86-21-65589829; E-mail: xiazhaofan_smmu@163.com

References

[1] Wu Y, Chen L, Scott PG and Tredget EE. Mesenchymal stem cells enhance wound healing through differentiation and angiogenesis. Stem Cells 2007; 25: 2648-2659.

[2] Gurtner GC, Werner S, Barrandon Y and Longaker MT. Wound repair and regeneration. Nature 2008; 453: 314-321.

[3] Vernon RB, Preisinger A, Gooden MD, D'Amico LA, Yue BB, Bollyky PL, Kuhr CS, Hefty TR, Nepom GT and Gebe JA. Reversal of diabetes in mice with a bioengineered islet implant incorporating a type I collagen hydrogel and sustained release of vascular endothelial growth factor. Cell Transplant 2012; 21: 2099-2110.

[4] Zhang YQ, Ji SZ, Fang H, Zheng YJ, Luo PF, Wu HB, Wu MJ, Wang ZH, Xiao SC and Xia ZF. Use of amniotic microparticles coated with fibroblasts overexpressing SDF-1alpha to create an environment conducive to neovascularization for repair of full-thickness skin defects. Cell Transplant 2016; 25: 365-376.

[5] Gonzalez AC, Costa TF, Andrade ZA and Medrado AR. Wound healing - a literature review. An Bras Dermatol 2016; 91: 614-620.

[6] Behm B, Babilas P, Landthaler M and Schreml S. Cytokines, chemokines and growth factors in wound healing. J Eur Acad Dermatol Venereol 2012; 26: 812-820.

[7] Acevedo L, Yu J, Erdjument-Bromage H, Miao RQ, Kim JE, Fulton D, Tempst P, Strittmatter SM and Sessa WC. A new role for Nogo as a regulator of vascular remodeling. Nat Med 2004; 10: 382-388.

[8] Gao L, Utsumi T, Tashiro K, Liu B, Zhang D, Swenson ES and Iwakiri Y. Reticulon 4B (Nogo-B) facilitates hepatocyte proliferation and liver regeneration in mice. Hepatology 2013; 57: 1992-2003.

[9] Xu W, Zhu Y, Ning Y, Dong Y, Huang H, Zhang W, Sun Q and Li Q. Nogo-B protects mice against lipopolysaccharide-induced acute lung injury. Sci Rep 2015; 5: 12061.

[10] Yu J, Fernandez-Hernando C, Suarez Y, Schleicher M, Hao Z, Wright PL, DiLorenzo A, Kyriakides TR and Sessa WC. Reticulon 4B (Nogo-B) is necessary for macrophage infiltration and tissue repair. Proc Natl Acad Sci U S A 2009; 106: 17511-17516.

[11] Galiano RD, Michaels JT, Dobryansky M, Levine JP and Gurtner GC. Quantitative and reproducible murine model of excisional wound healing. Wound Repair Regen 2004; 12: 485-492.

[12] Xiao W, Zhou S, Xu H, Li H, He G, Liu Y and Qi Y. Nogo-B promotes the epithelial-mesenchymal transition in HeLa cervical cancer cells via Fibulin-5. Oncol Rep 2013; 29: 109-116.

[13] Pula B, Werynska B, Olbromski M, Muszczynska-Bernhard B, Chabowski M, Janczak D, Zabel M, Podhorska-Okolow M and Dziegiel P. Expression of Nogo isoforms and Nogo-B receptor (NgBR) in non-small cell lung carcinomas. Anticancer Res 2014; 34: 4059-4068.

[14] Dong C, Zhao B, Long F, Liu Y, Liu Z, Li S, Yang X, Sun D, Wang H, Liu Q, Liang R, Li Y, Gao Z, Shao S, Miao QR and Wang L. Nogo-B receptor promotes the chemoresistance of human hepatocellular carcinoma via the ubiquitination of p53 protein. Oncotarget 2016; 7: 8850-8865.

[15] Calik J, Pula B, Piotrowska A, Wojnar A, Witkiewicz W, Grzegrzolka J, Podhorska-Okolow M and Dziegiel P. Prognostic significance of NOGO-A/B and NOGO-B receptor expression in malignant melanoma - a preliminary study. Anticancer Res 2016; 36: 3401-3407.

[16] Cantalupo A, Zhang Y, Kothiya M, Galvani S, Obinata H, Bucci M, Giordano FJ, Jiang XC and Hla T. Nogo-B regulates endothelial sphingolipid homeostasis to control vascular function and blood pressure. Nat Med 2015; 21: 1028-1037.

[17] Zhang Y, Huang Y, Cantalupo A, Azevedo PS, Siragusa M, Bielawski J, Giordano FJ and Di Lorenzo A. Endothelial Nogo-B regulates sphingolipid biosynthesis to promote pathological cardiac hypertrophy during chronic pressure overload. JCI Insight 2016; 1.

[18] Rodriguez-Feo JA, Gallego-Delgado J, Puerto M, Wandosell F and Osende J. Reticulon-4B/Nogo-B acts as a molecular linker between microtubules and actin cytoskeleton in vascular smooth muscle cells. Biochim Biophys Acta 2016; 1863: 1985-1995.

[19] Pan JW, Zheng X, Yang PY, Qin YW, Rui YC, Ma LP, Zhou F and Kang H. Different expressions of Nogo-B1 and Nogo-B2 in mouse heart microvascular endothelial cell dysfunction induced by lysophosphatidylcholine. Microvasc Res 2006; 72: 42-47.

[20] Wen M, Men R, Yang Z, Dan X, Wu W, Liu X and Yang L. The value of circulating Nogo-B for evaluating hepatic functional reserve in patients with cirrhosis. Dis Markers 2015; 2015: 419124.

[21] Tashiro K, Satoh A, Utsumi T, Chung C and Iwakiri Y. Absence of Nogo-B (reticulon 4B) facilitates hepatic stellate cell apoptosis and diminishes hepatic fibrosis in mice. Am J Pathol 2013; 182: 786-795.

[22] Men R, Wen M, Dan X, Zhu Y, Wang W, Li J, Wu W, Liu X and Yang L. Nogo-B: a potential indicator for hepatic cirrhosis and regulator in hepatic stellate cell activation. Hepatol Res 2015; 45: 113-122.

[23] Hu W, Zhang W, Chen Y, Rana U, Teng RJ, Duan Y, Liu Z, Zhao B, Foeckler J, Weiler H, Kallinger RE, Thomas MJ, Zhang K, Han J and Miao QR. Nogo-B receptor deficiency increases LXRal-

pha nuclear translocation and hepatic lipogenesis via an AMPKalpha-dependent pathway. Hepatology 2016; 64: 1559-1576.
[24] Di Lorenzo A, Xu W, Zhu Y, Ning Y, Dong Y, Huang H, Zhang W, Sun Q and Li Q. Nogo-B protects mice against lipopolysaccharide-induced acute lung injury. Nat Med 2015; 5: 12061.
[25] Wright PL, Yu J, Di YP, Homer RJ, Chupp G, Elias JA, Cohn L and Sessa WC. Epithelial reticulon 4B (Nogo-B) is an endogenous regulator of Th2-driven lung inflammation. J Exp Med 2010; 207: 2595-2607.
[26] Marin EP, Moeckel G, Al-Lamki R, Bradley J, Yan Q, Wang T, Wright PL, Yu J and Sessa WC. Identification and regulation of reticulon 4B (Nogo-B) in renal tubular epithelial cells. Am J Pathol 2010; 177: 2765-2773.
[27] Laschke MW, Harder Y, Amon M, Martin I, Farhadi J, Ring A, Torio-Padron N, Schramm R, Rucker M, Junker D, Haufel JM, Carvalho C, Heberer M, Germann G, Vollmar B and Menger MD. Angiogenesis in tissue engineering: breathing life into constructed tissue substitutes. Tissue Eng 2006; 12: 2093-2104.
[28] Zheng Y, Ji S, Wu H, Tian S, Wang X, Luo P, Fang H, Wang Z, Wang J, Wang Z, Xiao S and Xia Z. Acceleration of diabetic wound healing by a cryopreserved living dermal substitute created by micronized amnion seeded with fibroblasts. Am J Transl Res 2015; 7: 2683-2693.
[29] Griffith CK, Miller C, Sainson RC, Calvert JW, Jeon NL, Hughes CC and George SC. Diffusion limits of an in vitro thick prevascularized tissue. Tissue Eng 2005; 11: 257-266.
[30] Toh H, Cao M, Daniels E and Bateman A. Expression of the growth factor progranulin in endothelial cells influences growth and development of blood vessels: a novel mouse model. PLoS One 2013; 8: e64989.
[31] He Z, Ong CH, Halper J and Bateman A. Progranulin is a mediator of the wound response. Nat Med 2003; 9: 225-229.
[32] Brauer R, Beck IM, Roderfeld M, Roeb E and Sedlacek R. Matrix metalloproteinase-19 inhibits growth of endothelial cells by generating angiostatin-like fragments from plasminogen. BMC Biochem 2011; 12: 38.
[33] Huang CC, Pan WY, Tseng MT, Lin KJ, Yang YP, Tsai HW, Hwang SM, Chang Y, Wei HJ and Sung HW. Enhancement of cell adhesion, retention, and survival of HUVEC/cbMSC aggregates that are transplanted in ischemic tissues by concurrent delivery of an antioxidant for therapeutic angiogenesis. Biomaterials 2016; 74: 53-63.